Introduction to Tomography

- **Tomography** is imaging by sections or sectioning. A device used in tomography is called a **tomograph**, while the image produced is a **tomogram**.
- The method is used in medicine, archaeology, biology, geophysics, oceanography, materials science, astrophysics and other sciences.
- In most cases it is based on the mathematical procedure called **tomographic reconstruction**.
- The word "tomography" is derived from the Greek *tomos* (slice) and *graphein* (to write).

Wickipedia

Introduction to Tomography

- **(projection) Tomography** is a method in which a 3-D structure is reconstructed from a series of 2-D projections (images) acquired at successive tilts (Radon 1917).
- First developed for use in medical imaging (1963, Nobel Prize for Medicine in 1979) using X-rays, ultrasound and magnetic resonance (e.g. 'cat-scans')..
- Found further application in geology, astronomy, materials science, etc…

P. Midgley, tomo workshop in Berlin

Introduction to Tomography

Recording

- Series of 2D images
  direct tomography:
  serial sections
  projection tomography
  projections in different diretions
- Destructive: serial sectioning, FIB, AP
- Non-destructive:
  X-rays, TEM

Reconstruction and « viewing »

- Registration (alignment of images)
- Back-projection, reconstruction (tilt-series)
- **Tomogram:**
  stack of images
- Segmentation (image processing): extraction and visualisation of the desired information

Example: « direct » tomography FIB Nanotomography

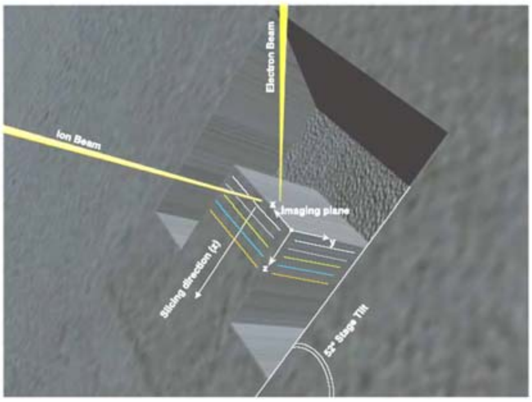

The FIB as a 3-D microscope:
Combine the milling possibility with imaging capabilities.

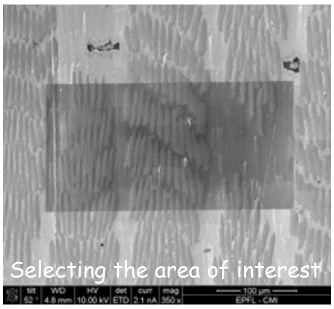

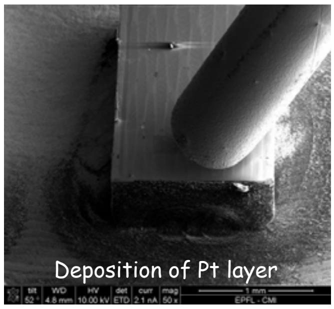

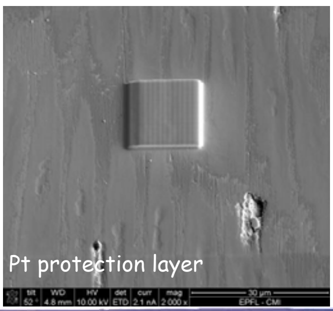

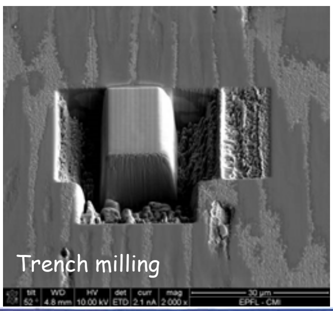

3D FIB/SEM: volume reconstruction

Nb_3Sn multifilament superconducting cable

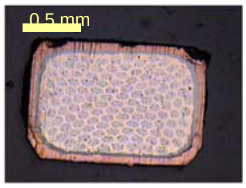

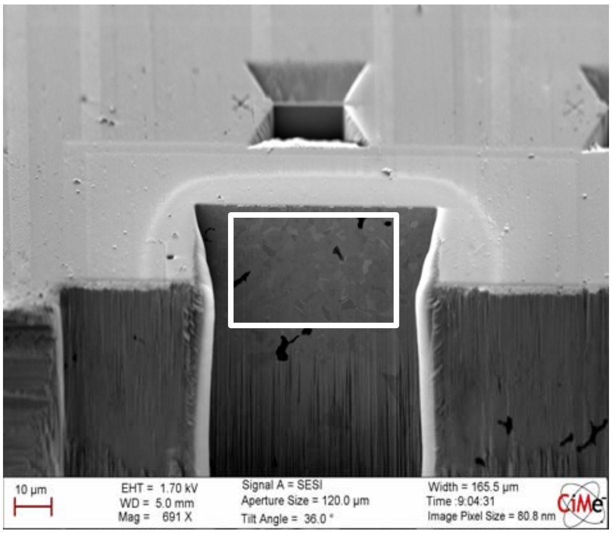

Nb_3Sn superconductor multifilament cable: 14'000 Nb_3Sn filaments (diameter ~5um) in Cu matrix

Preparing for automated milling, selection of area of interest

3D FIB/SEM: volume reconstruction

Nb_3Sn multifilament superconducting cable

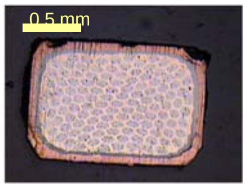

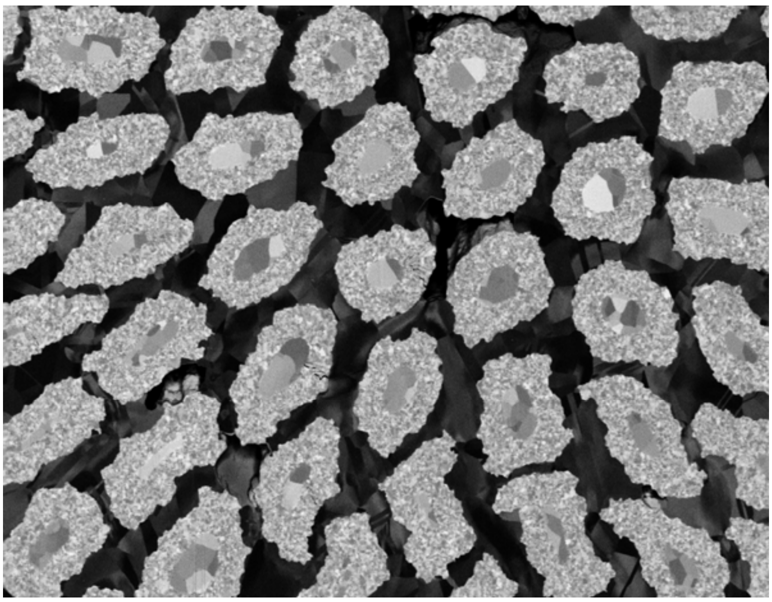

Nb_3Sn superconductor multifilament cable: 14'000 Nb_3Sn filaments (diameter ~5um) in Cu matrix

Finding the optimal imaging conditions

1.8kV EsB detector: Materials & orientation contrast

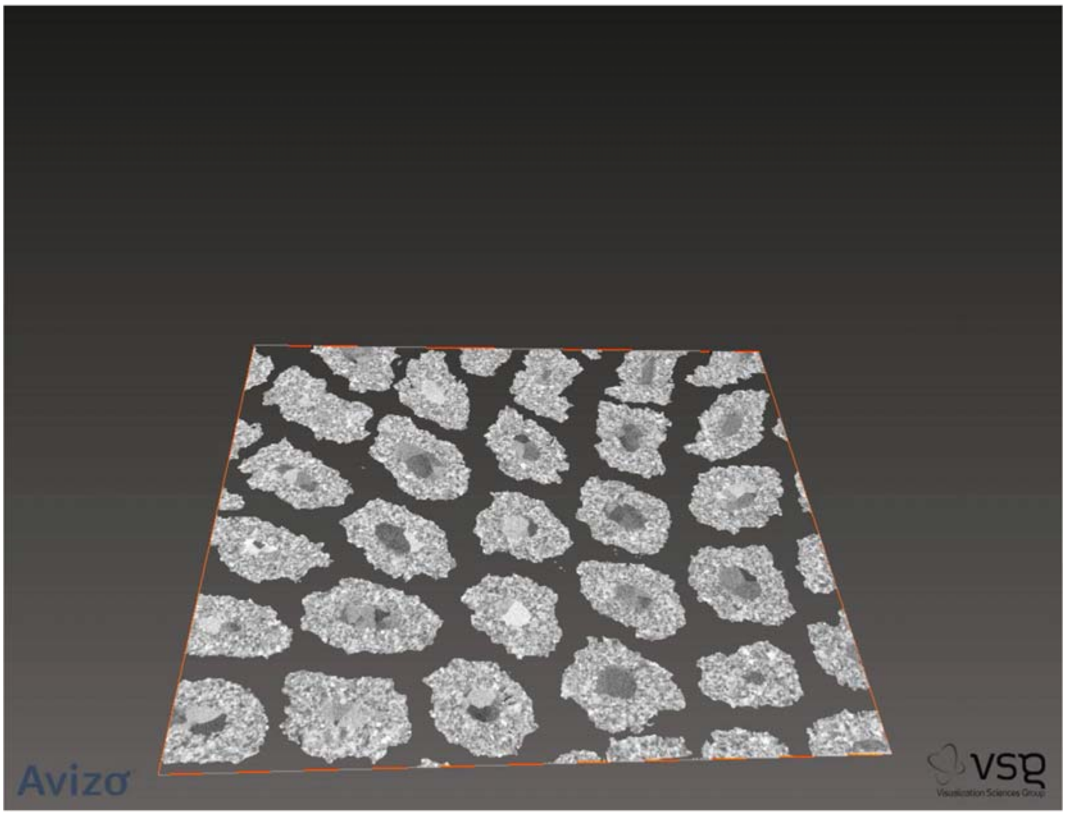

Materials & grain contrast

2048x1536x1700, (10x10x10nm voxel), 28hours

FIB-NT compared with other 3D-techniques

- isotropic voxel size ~5-10nm
- Dwell time ~5-10μsec.
- 1 slice, image / min.
- HT: 1-2kV
- Escape depth of signal (BSE) ≤ 5nm

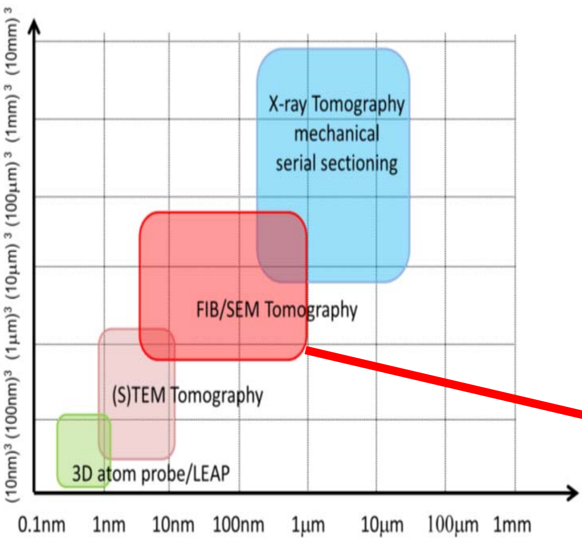

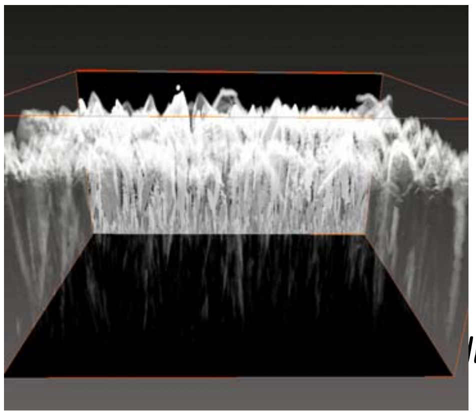

New possibilities in 3D-microscopy: Combination with quantitative analytical SEM techniques: EBSD, EDX

Focused ion beam

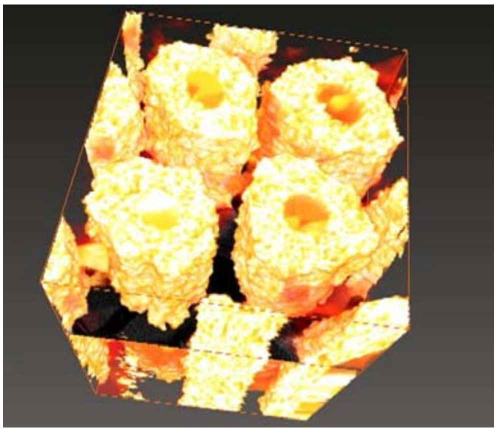

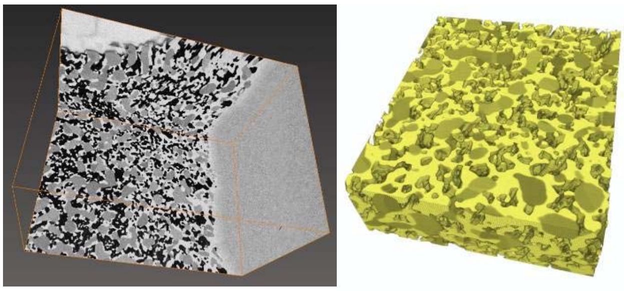

SOFC electrode material, (porous Ni-CGO anode)
2048x1536x1500, (12x12x12nm voxel)

Nb3Sn superconductor filaments:
2048x1536 pixels, 1700 slices
(10x10x10nm voxel), only small
fraction shown

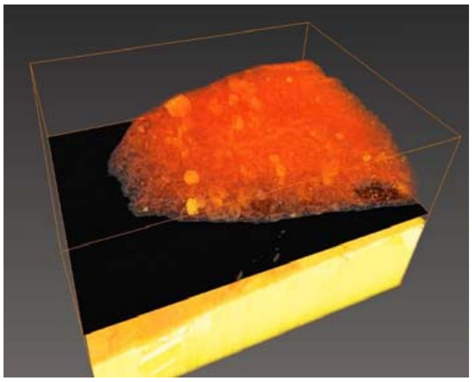

FIB-Nanotomography

Cell on substrate: 2048x1536x600
(10x10x20nm voxel), 20x15x12 microns

3D imaging in medicine

- Non-invasive methods are preferred!
- The disadvantage of conventional X-radiographs is its inability to discriminate between organs of close absorptivity or overlapping organs in the viewing direction.
- X-ray computed tomography overcomes that limitation:
- X-radiographs are made in many different directions and combined mathematically to to reconstruct cross-sectional maps.
- reconstruction tomography or computer assisted tomography.

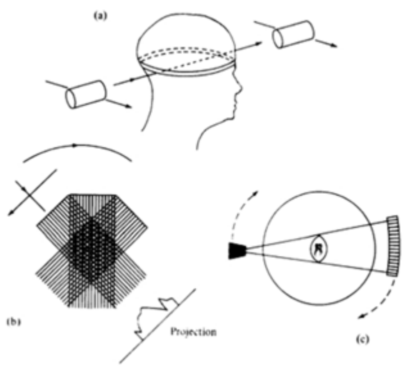

Tomograph

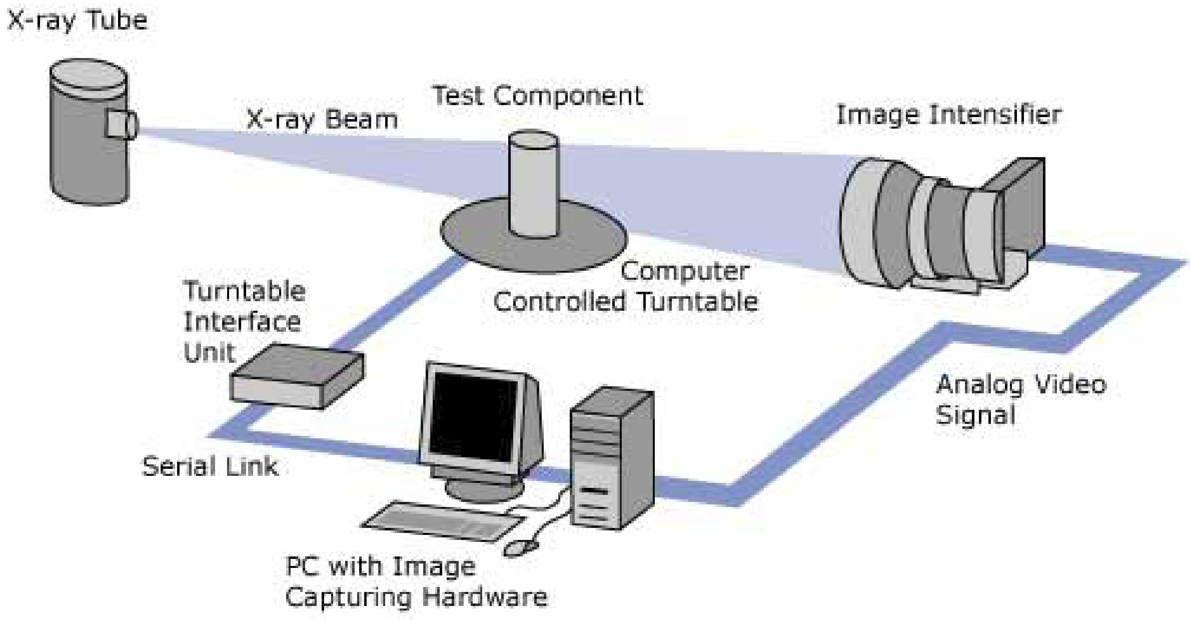

Radon 1917

Über die Bestimmung von Funktionen durch ihre Integralwerte längs gewisser Mannigfaltigkeiten.

Von

Johann Radon.

Integriert man eine geeigneten Regularitätsbedingungen unterworfene Funktion zweier Veränderlichen x, y — eine *Punktfunktion* $f(P)$ in der Ebene — längs einer beliebigen Geraden g, so erhält man in den Integralwerten $F(g)$ eine *Geradenfunktion*. Das in Abschnitt A vorliegender Abhandlung gelöste Problem ist die Umkehrung dieser linearen Funktionaltransformation, d. h. es werden folgende Fragen beantwortet: kann jede, geeigneten Regularitätsbedingungen genügende Geradenfunktion auf diese Weise entstanden gedacht werden? Wenn ja, ist dann f durch F eindeutig bestimmt und wie kann es ermittelt werden?

Ber. Sächs. Akad. Wiss. Leipzig, Math. Phys. Kl. 69, 262 (1917)

English translation in: Deans, S.R. (1983) The Radon transform and its applications. John Wiley & Sons, NY)

Radon Transform

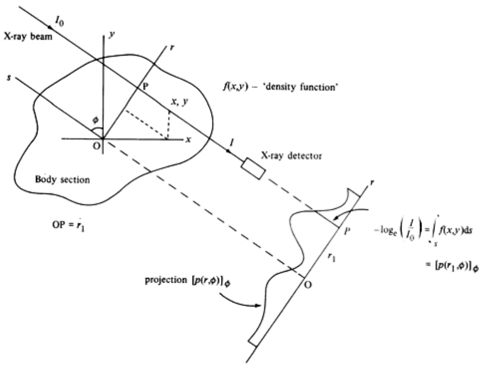

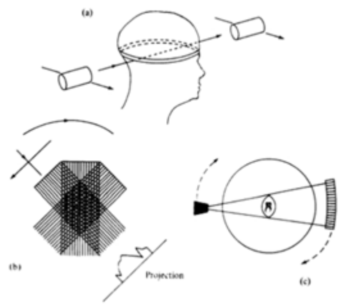

The paper defines the Radon transform *R* as the mapping of a function *f(x,y)*, describing a real space object *D*, by the projection, or line integral, through *f* along all possible lines *L*:

$$Rf = \int_L f(x,y)ds,$$

A discrete sampling of the Radon transform is geometrically equivalent to the sampling of an experimental object by some form of transmitted signal: a projection. ***The consequence of such equivalency is that the reconstruction of an object f(x,y) from projections Rf can be achieved by implementation of the inverse Radon transform***

Radon Transform

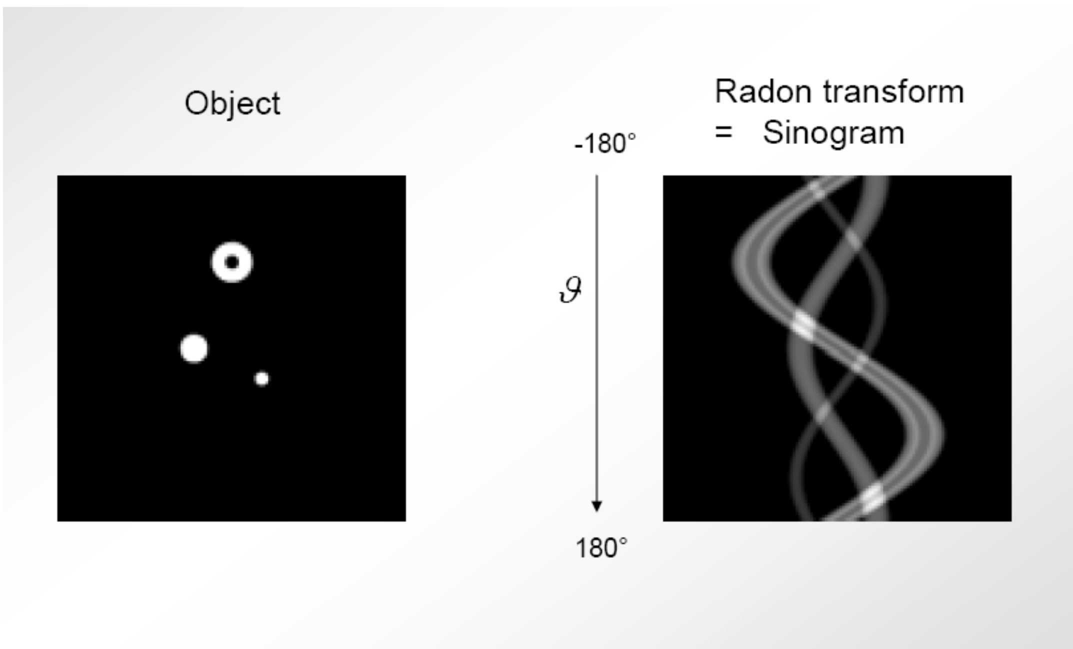

Radon Transform

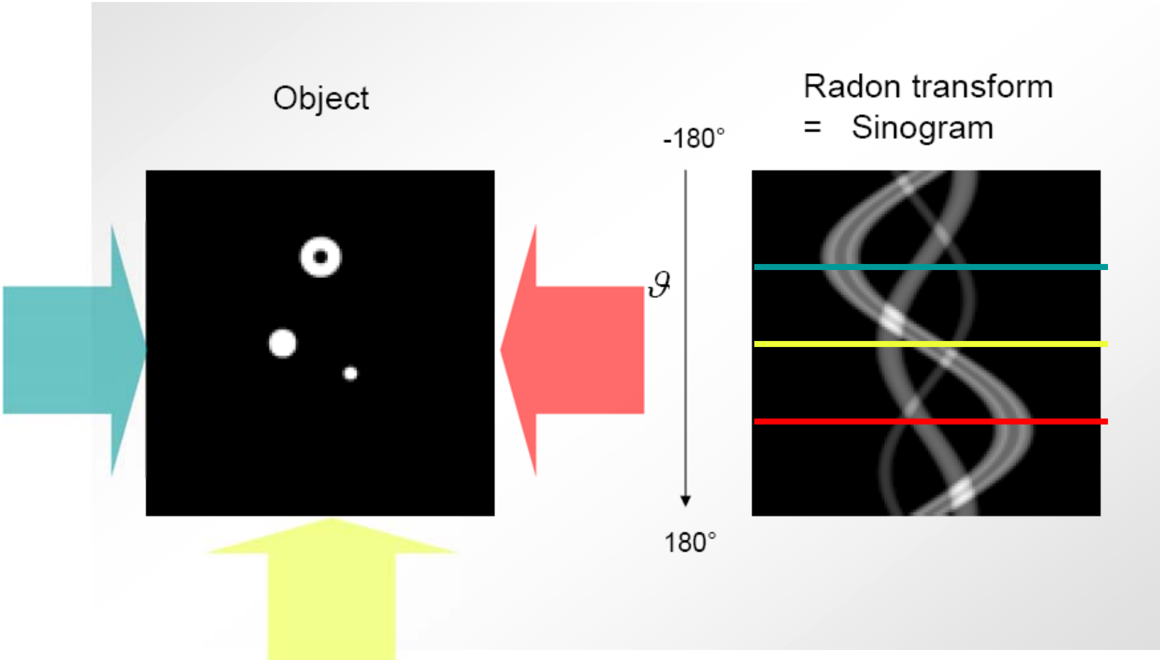

Back projection

"Reversing" of the projection process: usong the projected signal to "back-project" information.

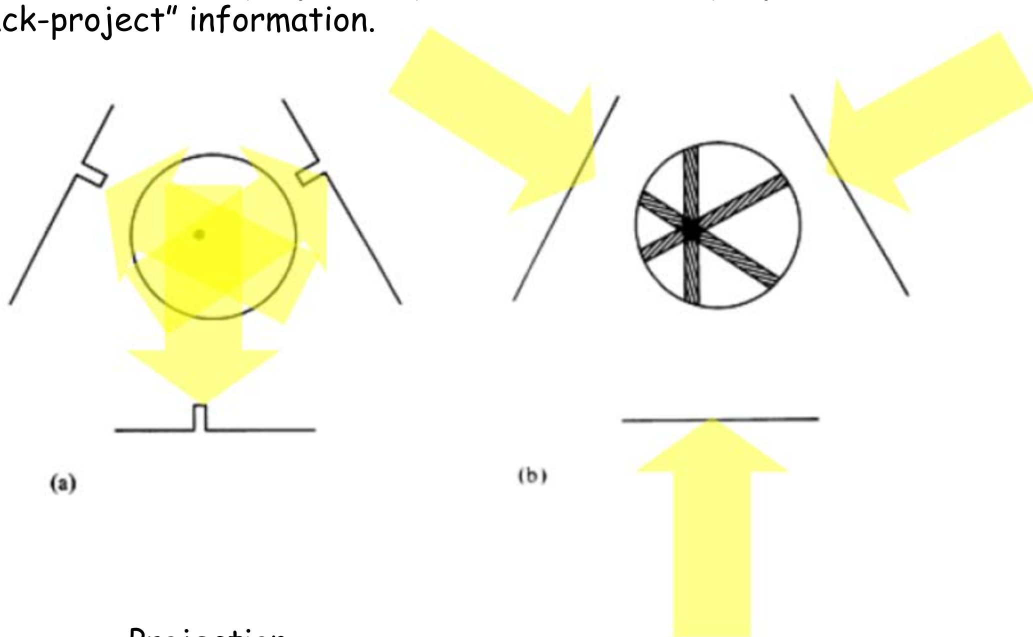

Projection recording

Back projection reconstructing

Back projection

The higher the number of projections the better will be the reconstructed object

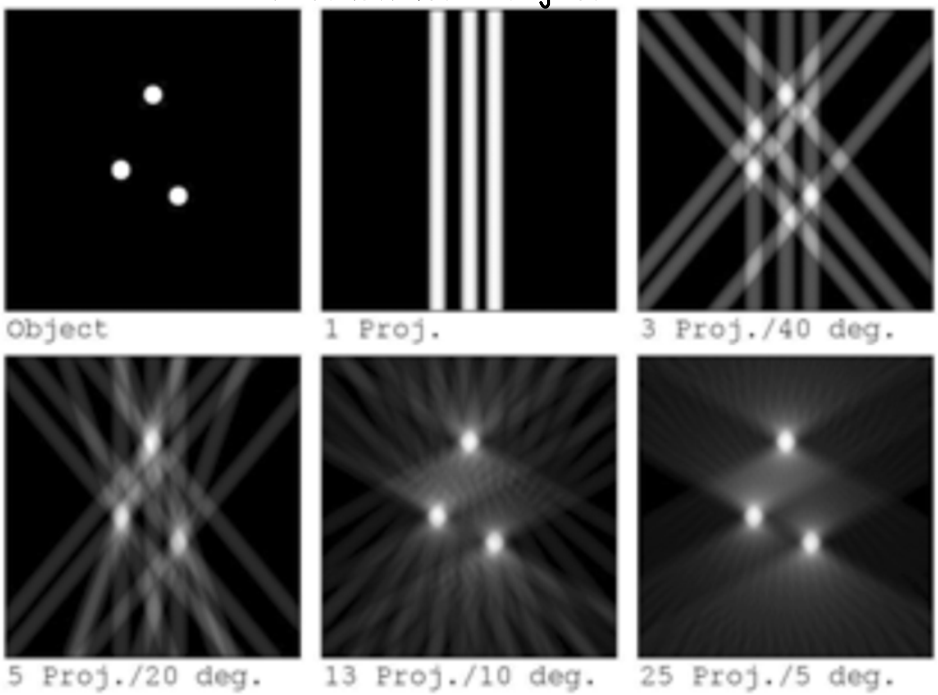

back projection

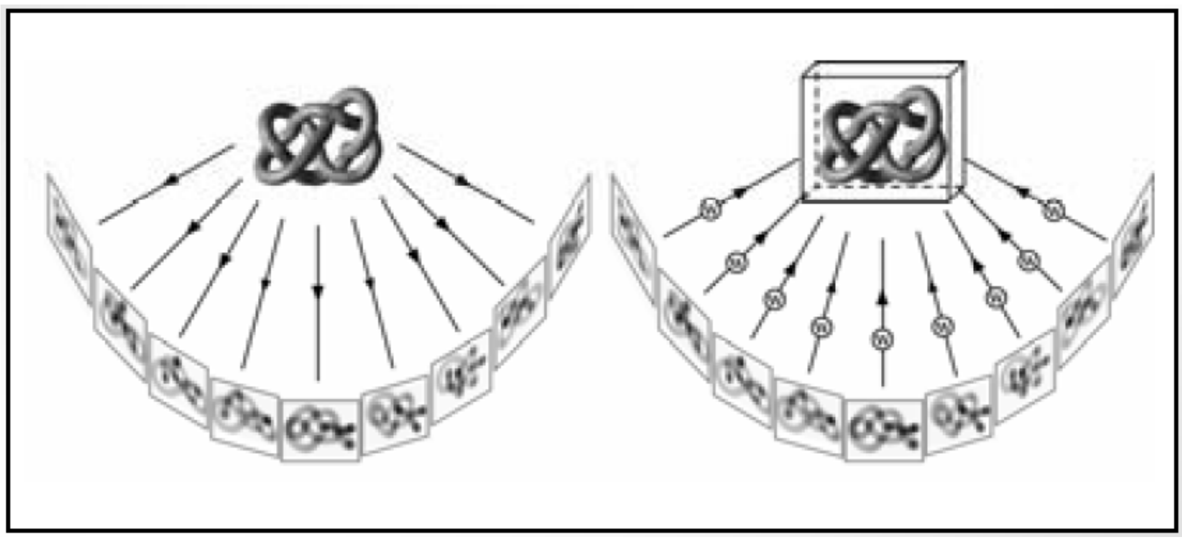

Tomography in medicine

3D imaging in materials science

360degree X-ray tomography
Milan Felberbaum
STI-IMX-LSMX

Cylinder of an Al-Cu Alloy

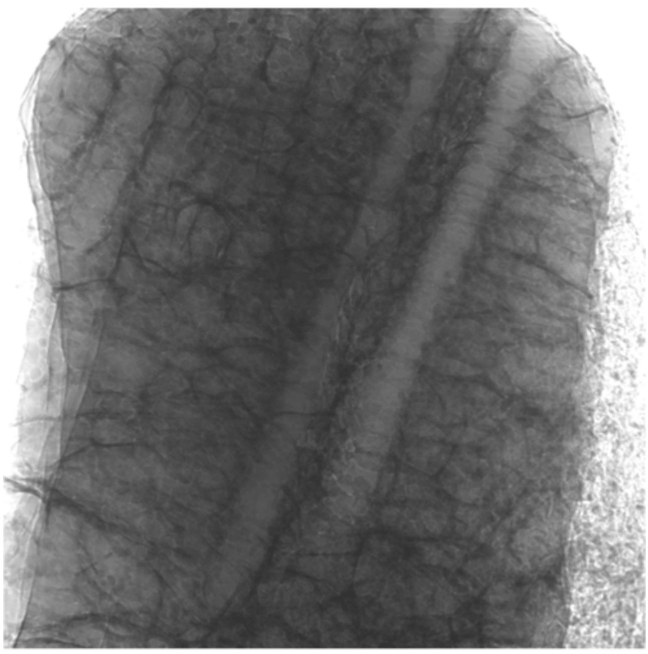

3D imaging in materials science

Tomogram

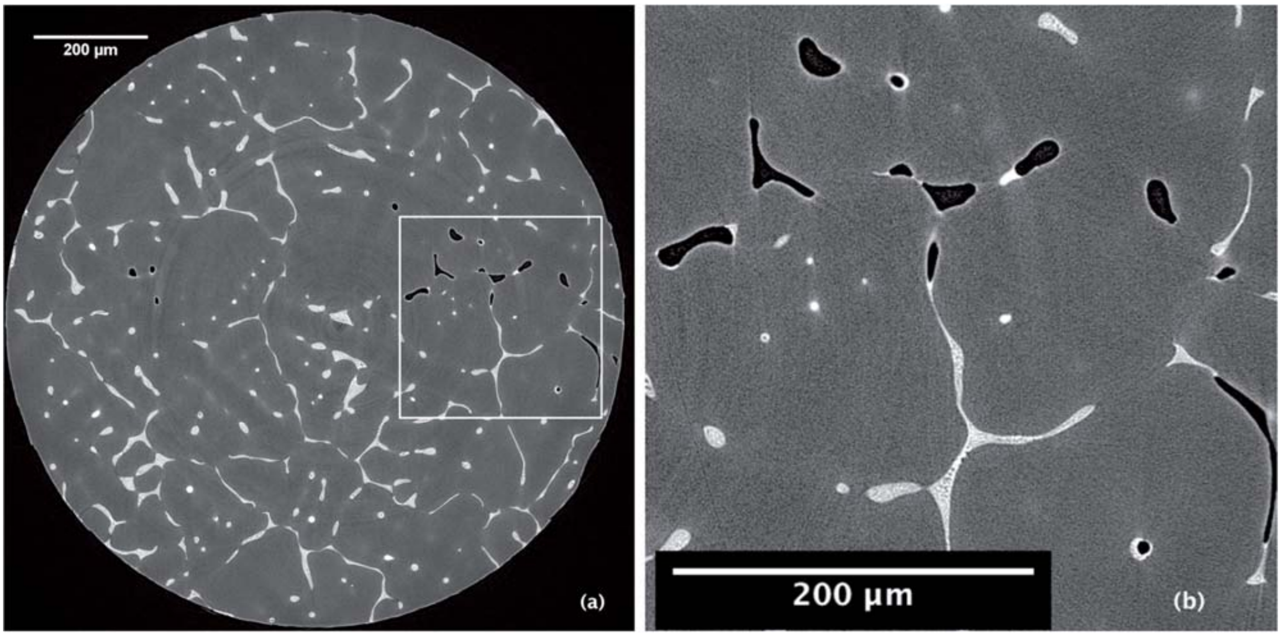

3D imaging in materials science

Reconstructed pore

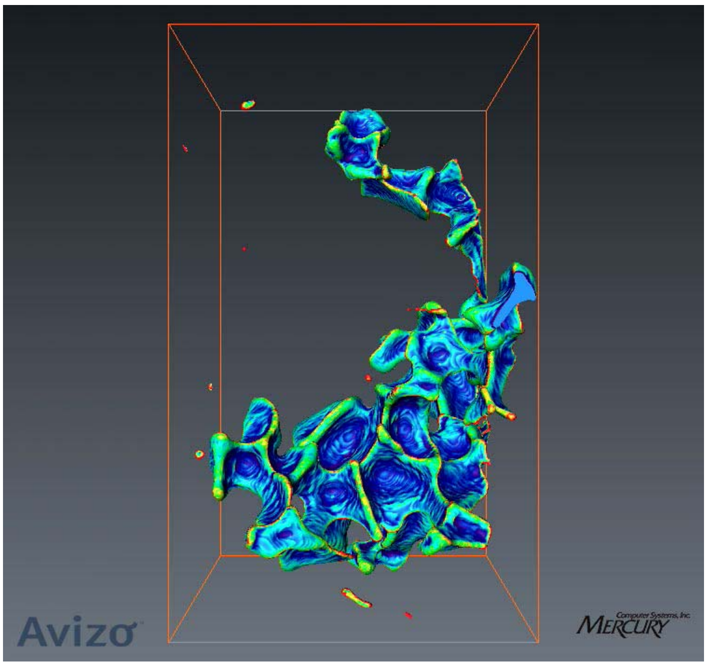

Tomography with electrons

higher resolution but lower penetration…

Stopping range for electrons (99% absorbed)

Element (specific weight)	4-Be 1.84 g/cm^3	13-Al 2.7 g/cm^3	29-Cu 8.93 g/cm^3	82-Pb 11.3 g/cm^3
X-rays Cu-Kα λ=1.54 Å Mo-Kα λ=0.71 Å	16 mm 83 mm	0.35 mm 3.3 mm	0.10 mm 0.10 mm	0.017 mm 0.034 mm
Neutrons λ≈1.08 Å	89 m	6 m	0.26 m	14 m
Électrons λ=0.037 Å à 100 kV λ=0.020 Å à 300 kV	39 μm	42 μm ~330 μm	11 μm	0.6 μm

Bio-EM, Tomography

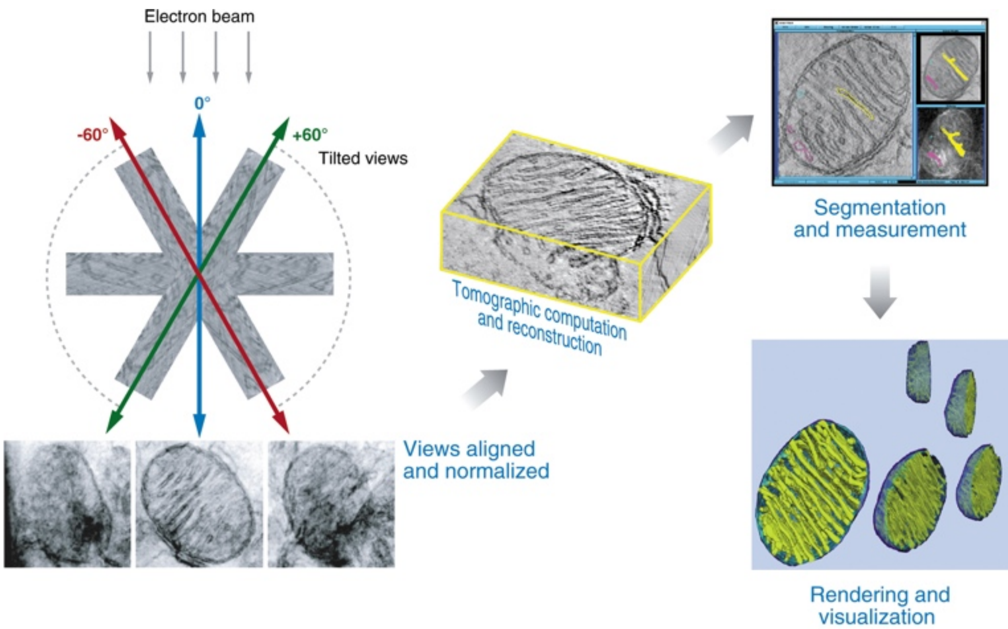

Frey TG, et al. 2006.
Annu. Rev. Biophys. Biomol. Struct. 35:199–224

Tilt series, -60 … +60 degree tilt

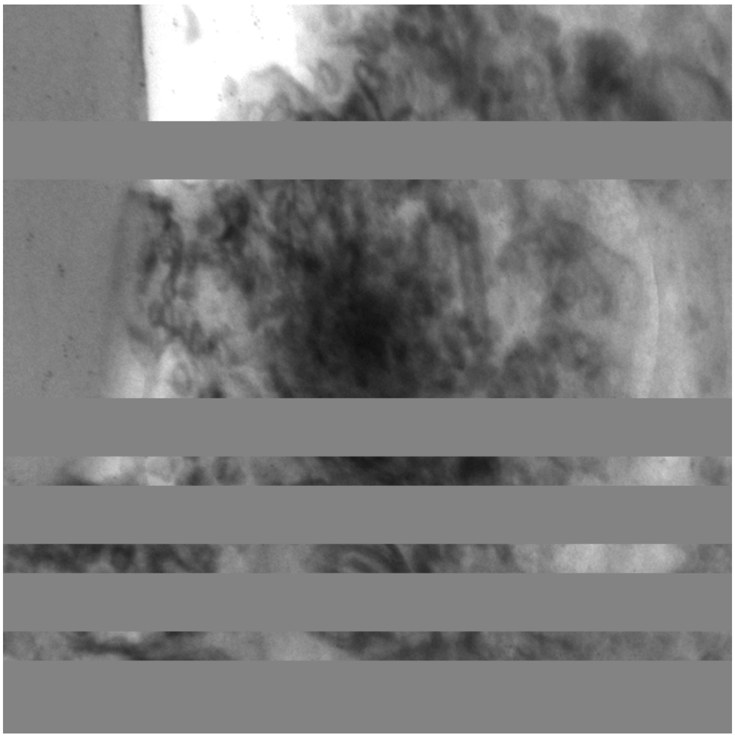

Tomogram

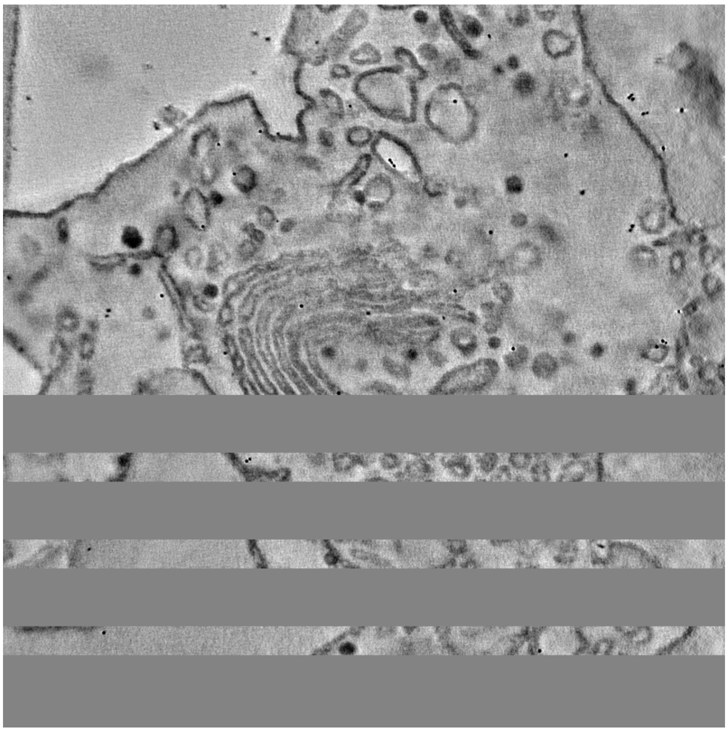

Tomo workflow

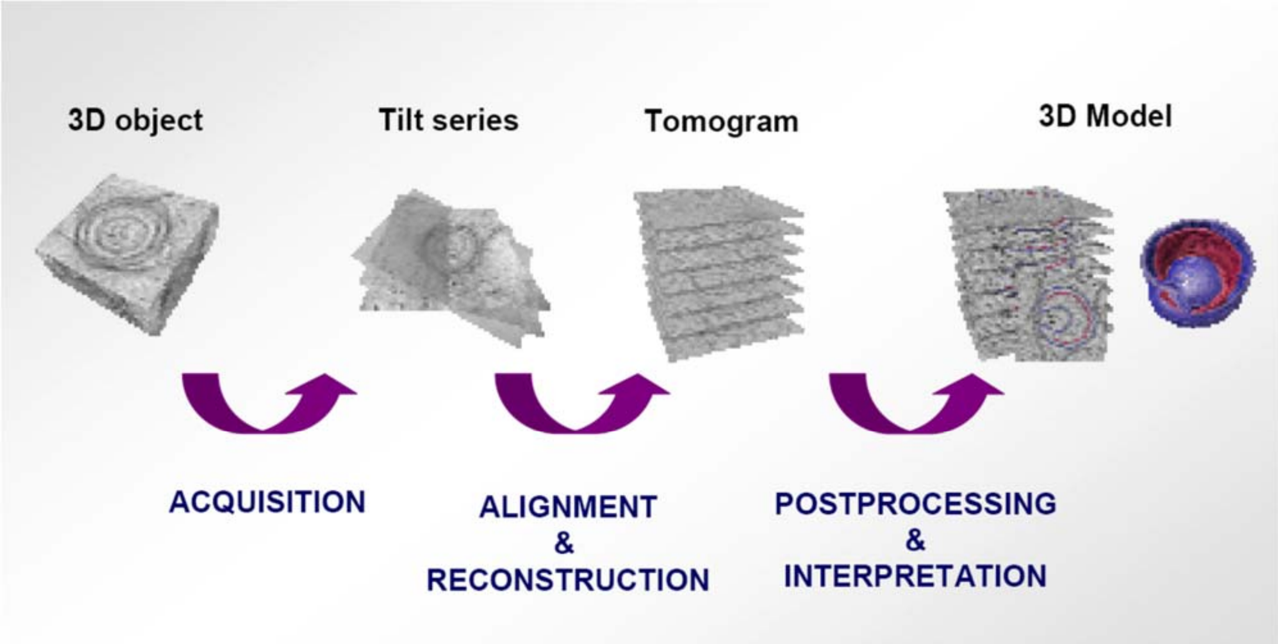

resolution

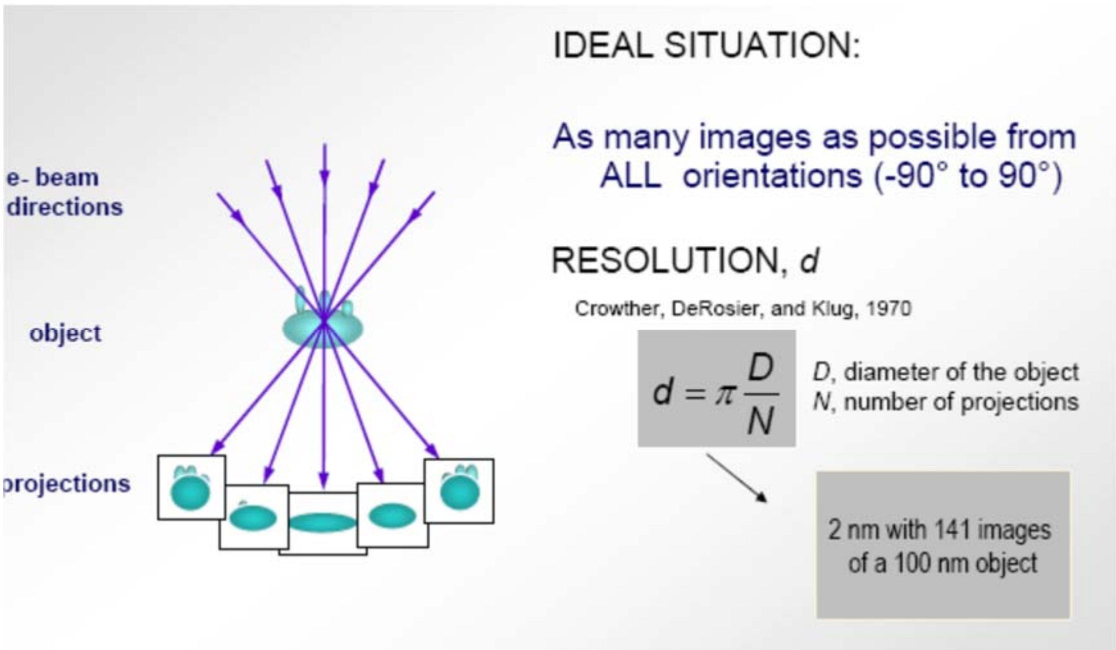

geometrical limit, the missing wedge

- There is a limit in the tilt angle we can reach (~±70°) due to:
  - Design of the holder
  - Grid bars
  - Increasing thickness of the specimen with high tilt angles

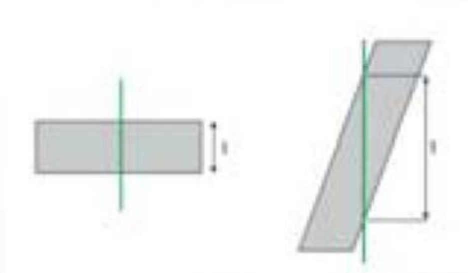

- This is known as the missing wedge problem (missing information, loss of resolution)

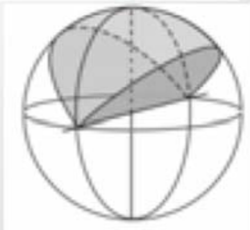

projection requirement

- projection requirement: monotonically varying function of a physical property: mass-thickness dominant in biological samples !

Diffraction contrast of crystalline samples in bright field TEM not suitable for Tomography

Z-contrast in STEM (HAADF): Mass-density contrast, suitable for tomography

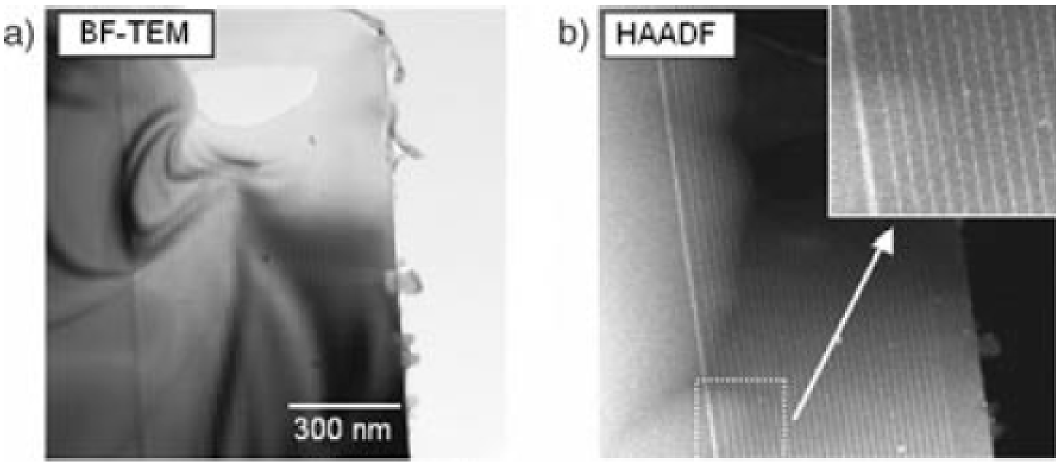

Si-Ge multiple quantum well structure

Tomography in Electron Microscopy

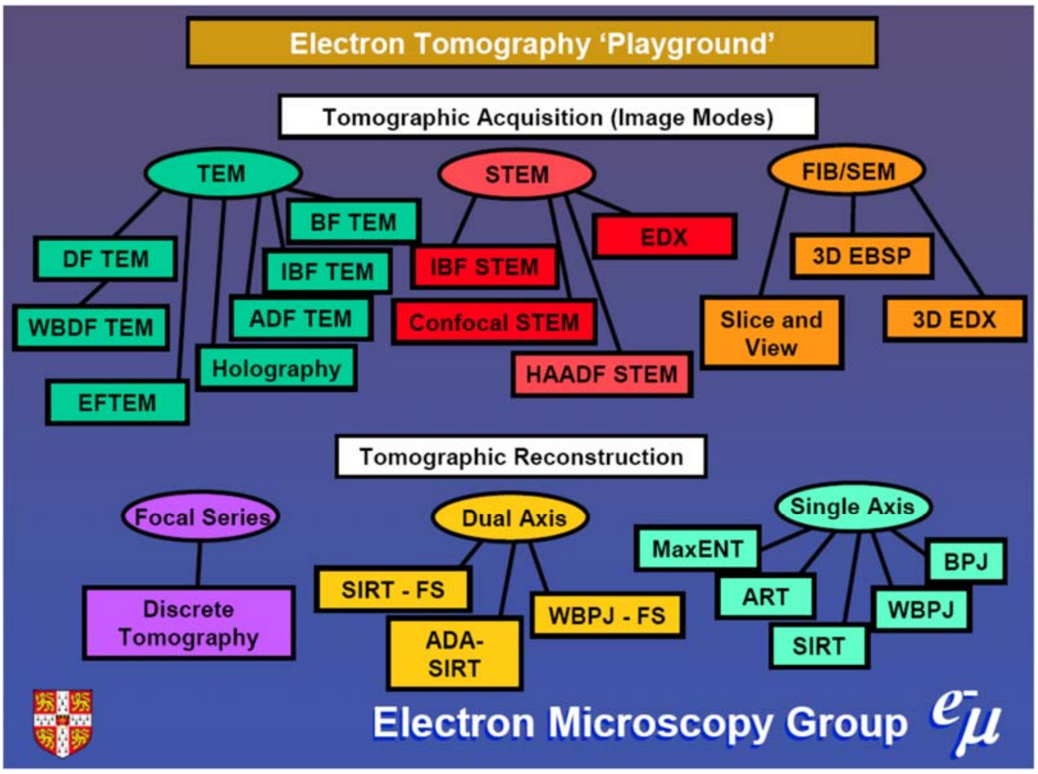

From P. Midgley

Tomography with HAADF (z-contrast)

nanoparticle bimetallic catalysts supported on mesoporous silica

Dogan Ozkaya,Paul Midgley; Catalysis Letters 60 (1999) 113–120

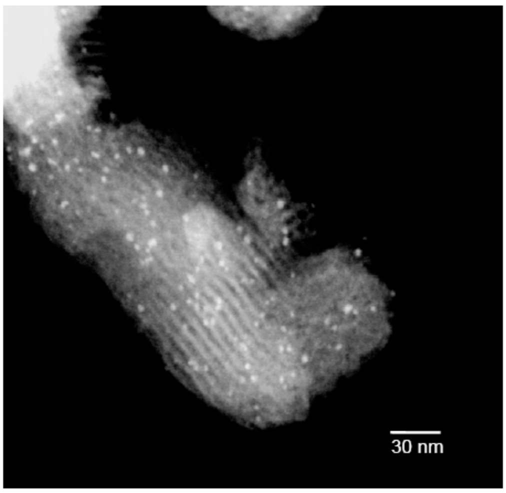

STEM HAADF: heterogeneous catalyst composed of Pd_6Ru_6 nanoparticles (~ 1 nm) on mesoporous silica support with mesopores of ~ 3 nm diameter.

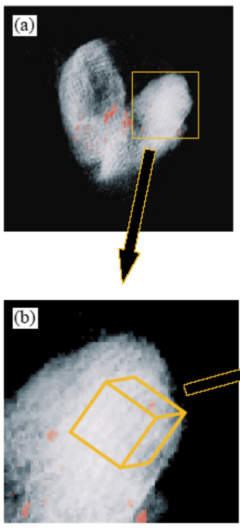

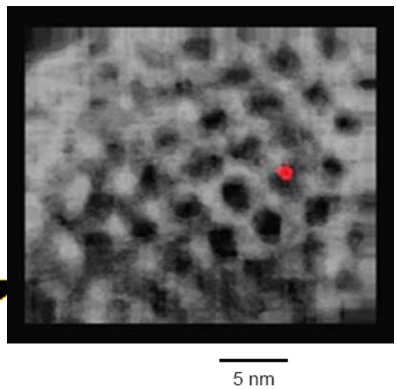

Pd_6Ru_6 nanoparticles anchored to the wall of mesopore

Electron Tomography in materials science

- Acquisition and alignment of 2x71 tilted images
- Back-projection: missing wedge
- Projection requirement (image contrast)
- Thickness limitation (samples rather thin)
- …
- …

Advanced 3D Technique

Atom Probe Tomography

Field emission (electron, ion) microscopy

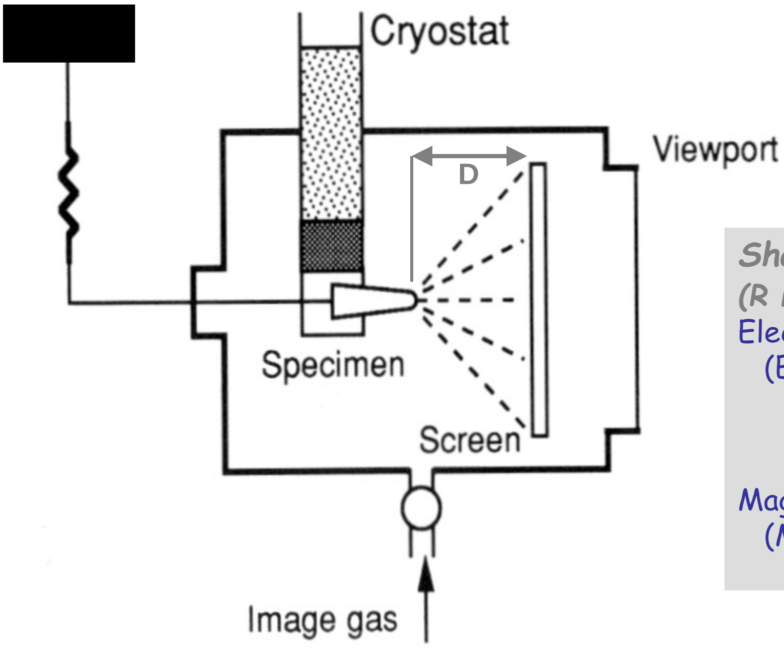

FEM: *vacuum*
HV<0

FIM: *low pressure rare gas*
HV>0

Sharp tip
(R radius of curvature):

Electric field ($E \approx 10^9$ V/m): $E = V/R$, $V \approx 1$ kV, $R \approx 0.1\ \mu m$

Magnification ($M \approx \ldots 10^6$): $M = D/R\beta$, $D \approx 0.3$ m, $\beta \approx 1.5$ (tip shape)

Field Ion Microscopy
Gas Field Ionisation Source (GFIS)

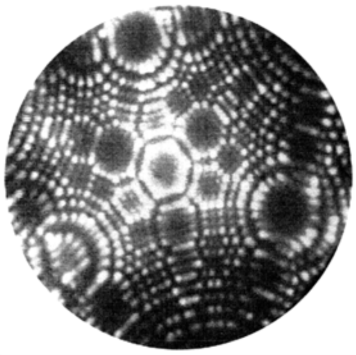

- atoms (molecules) are trapped by polarizations forces
- Trapped atoms hop on the surface until they are ionised

Ionisation: tunnelling process with probability D:

$$D \propto e^{\frac{-c(I-\Phi)}{V}}$$

I : Ionisation potential
Φ : Work function of emitter
V : El. Potential
c : constant

- Ions are ejected from the surface

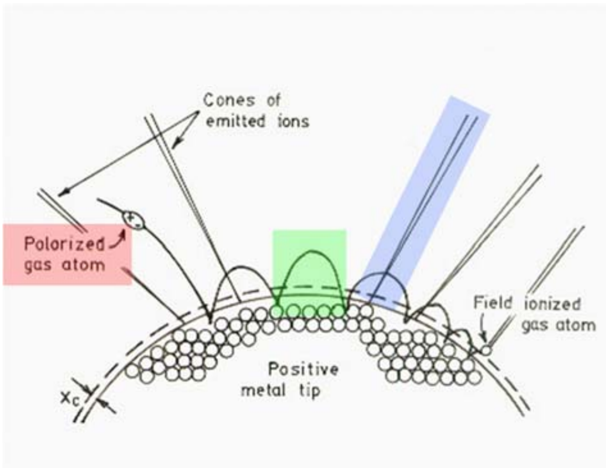

Field emission (electron, ion) microscopy *FEM, FIM*

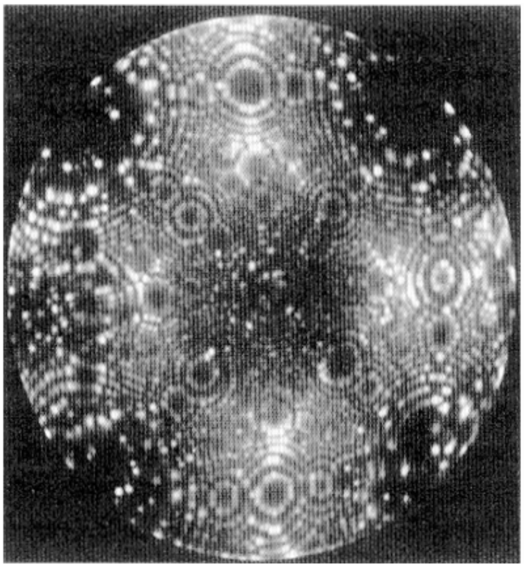

Field ion micrograph from a [100] oriented specimen of Pt 17 at.% Rh catalyst material imaged in Ne gas with an applied voltage of approx. 10 kV at 80K. Each of the bright spots in the left picture is the image of an individual atom on the specimen surface.

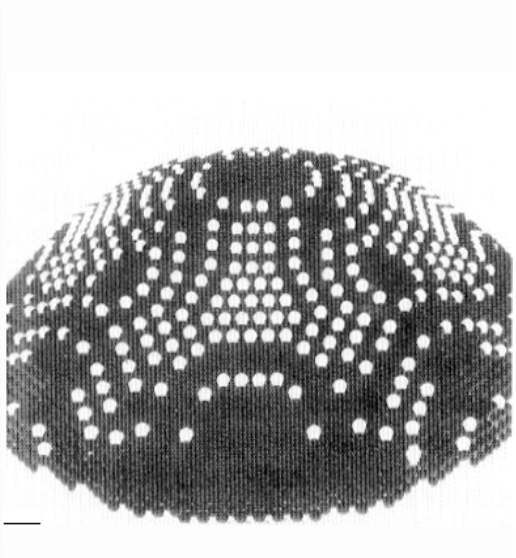

Ball model . The prominent sites, representing kink site atoms on the surface are shown in white. These form a serie of concentric rings similar to those seen in the field-ion picture

Atom probe Tomography

- Use the sample atoms as imaging ions….!
  - APFIM: Atom Probe Field Ion Microscopy
- Measure the Time Of Flight (TOF), to determine the mass of the ion…!
  - elemental analysis on atomic level
- Use Laser to assist ablation of ions
  - LAWATAP: Laser Assisted Wide Angle Tomographic Atom Probe
  - Insulating samples become possible

Wide Angle position sensitive detector

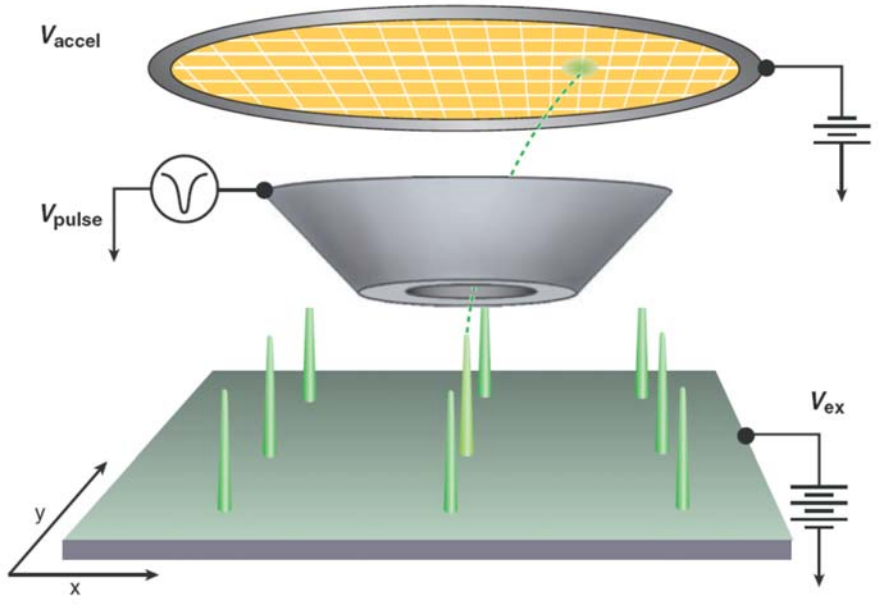

Sample needs to have tip shape: metals: etching, insulators: FIB

Annu. Rev. Mater. Res. 2007.37:127-158

Three-Dimensional Atom-Probe Tomography: Advances and Applications

David N. Seidman

Department of Materials Science and Engineering, Northwestern University Center for Atom-Probe Tomography, Northwestern University, Evanston, Illinois 60208-3108; email: d-seidman@northwestern.edu

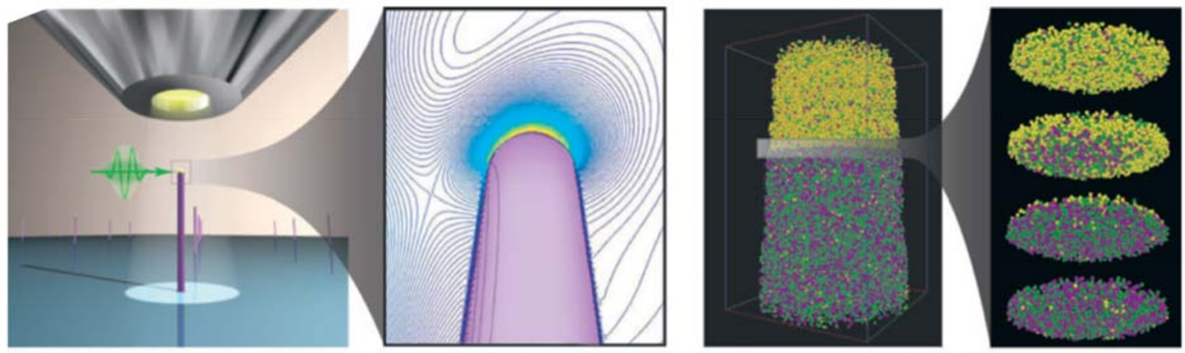

Figure 2

(Left) An array of microtips sitting on a conducting substrate with green laser light impinging on a single microtip. (Middle) The calculated electric field at a microtip that results from the **E**-component of the laser beam. Courtesy of Prof. Tamar Seideman (Chemistry Department, Northwestern University). (Right) The results of an analysis of an InAs nanowire grown by the vapor-liquid-solid (VLS) technique.

Detection speed

- **Electrical pulsing**
  The pulse repetition rate is variable in discrete steps from 1 kHz to 250 kHz, and a detection rate of up to 2×10^6 ion min−1 (120×10^6 ion h^{-1}) can be achieved. This implies that a data set containing 10^9 atoms can be obtained in 8 1/3 h from a single cooperative specimen. For electrical pulsing, the full-width half-maximum (FWHM) value of $m/\Delta m$ is 500.

- **Laser (picosecond) Pulsing**
  For the LEAP 3000X Si XTM, the laser pulse repetition rate is variable in steps from 1 kHz to 500 kHz, and a detection rate of up to 5×10^6 ion min−1 (300×10^6 ion h^{-1}) can be obtained. Therefore, a data set containing 10^9 atoms is attainable from a single very cooperative specimen in 3 1/3 h, which is a factor of 2.5 faster than with electrical pulsing.

Al–2.2 at.% Mg–0.12 at.% Sc alloy

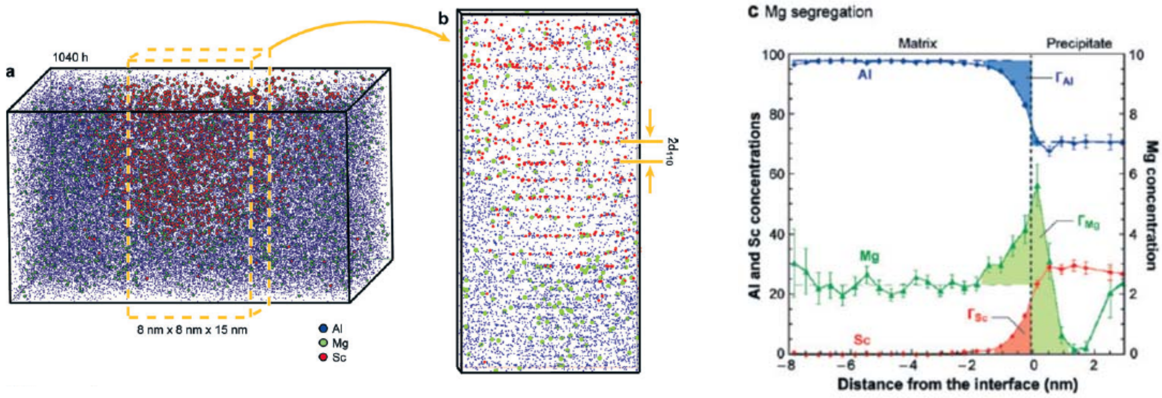

Figure 5

(*a*) 3-D reconstruction of an analyzed volume from a specimen aged at 300°C for 1040 h showing the isoconcentration surface used to define the α-Al/Al_3Sc heterophase interface. (*b*) 3-D reconstruction of an Al_3Sc precipitate with a slice taken through the precipitate displaying the {110} planes. (*c*) Proximity histogram showing Al, Mg, and Sc concentrations from the α-Al/Al_3Sc interface. Data visualization performed using Northwestern University's ADAM 1.5 software package (70). From Reference 86.

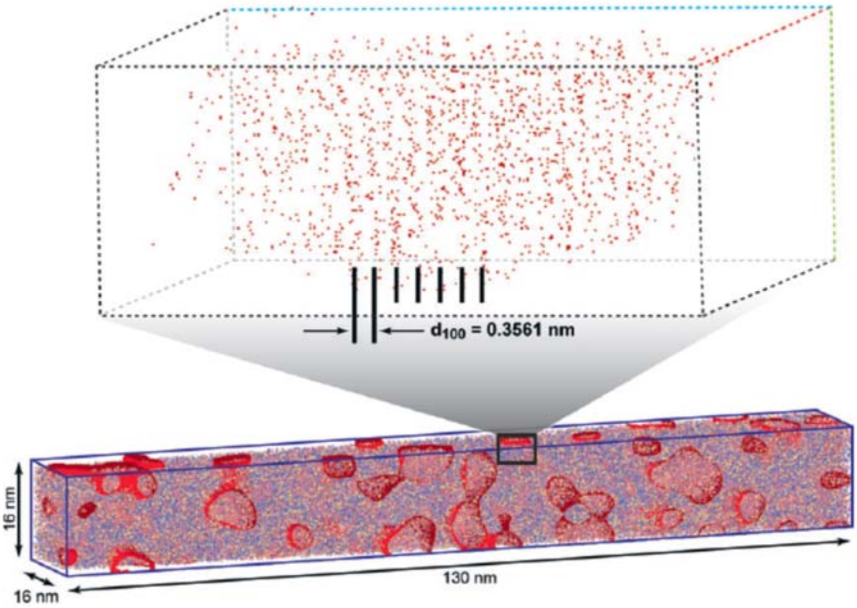

Figure 9

APT reconstruction of a Ni–10 at.% Al–8.5 at.% Cr–2 at.% Re alloy in the as-quenched state, which indicates the presence of γ'-precipitates. A 12 at.% Al isoconcentration surface is used to indicate the γ/γ' interfaces. A portion of the γ'-precipitate is magnified, with Al (*red*), Cr (*blue*), and Re (*orange*) atoms shown to display the alternating Al planes in the [100] direction of the ordered $L1_2$ structure. Ni atoms are not shown for the sake of clarity. Adapted from Reference 129.

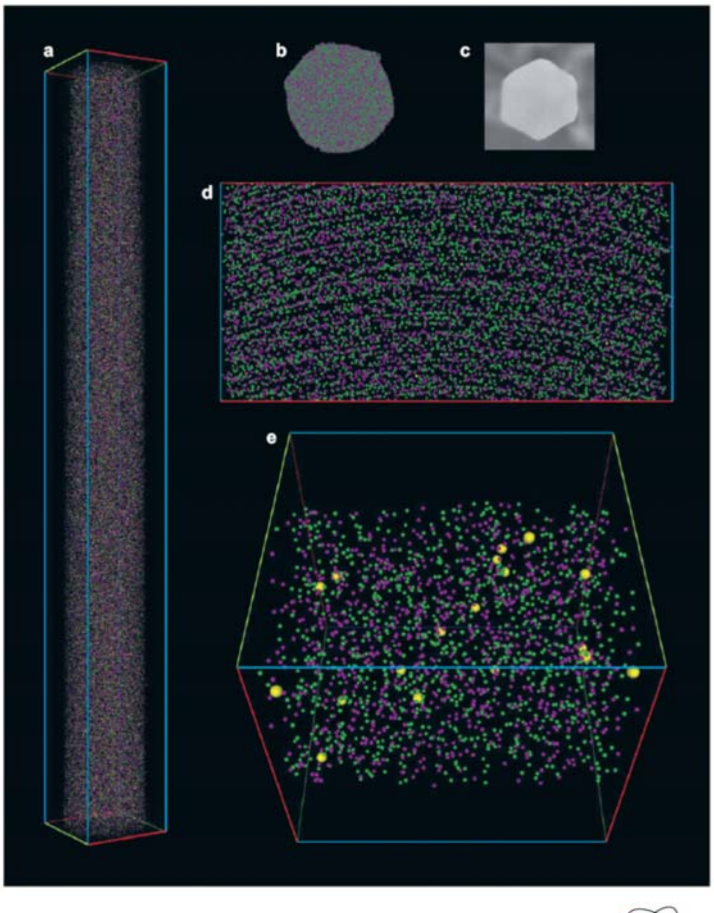

Figure 12

Three-dimensional reconstruction of an InAs nanowire. The sample temperature was at a fixed value between 50 K to 100 K, and the ambient pressure in the LEAP™ tomograph was 10^{-10} Torr during its atom-by-atom dissection. (*a*) Side view (perpendicular to growth axis) of a $25 \times 25 \times 300$ nm^3 reconstruction of the nanowire. In, As, and Au atoms are rendered as green, purple, and yellow dots, respectively. Only 5% of the atoms are displayed to provide a sense of depth. (*b*) A 21×21 nm^2 end-on view of nanowire reconstruction showing hexagonal faceting. (*c*) SEM micrograph of an InAs nanowire displaying a hexagonal cross section (1.7 μm^2). (*d*) Magnified side view of the nanowire displaying (0001) atomic planes. The dimensions are 23×14 nm^2. The slight curvature of the atomic planes is an artifact; the software used for the reconstruction assumes a hemispherical end-form for the field-evaporating nanowires. (*e*) For clarity, a $27 \times 27 \times 29$ nm^3 reconstruction of the nanowire with Au atoms is enlarged, and 2% of In and As atoms are shown; the growth axis runs left to right. The 18 Au atoms within the volume correspond to a concentration of 100 atomic parts per million. From Reference 121.

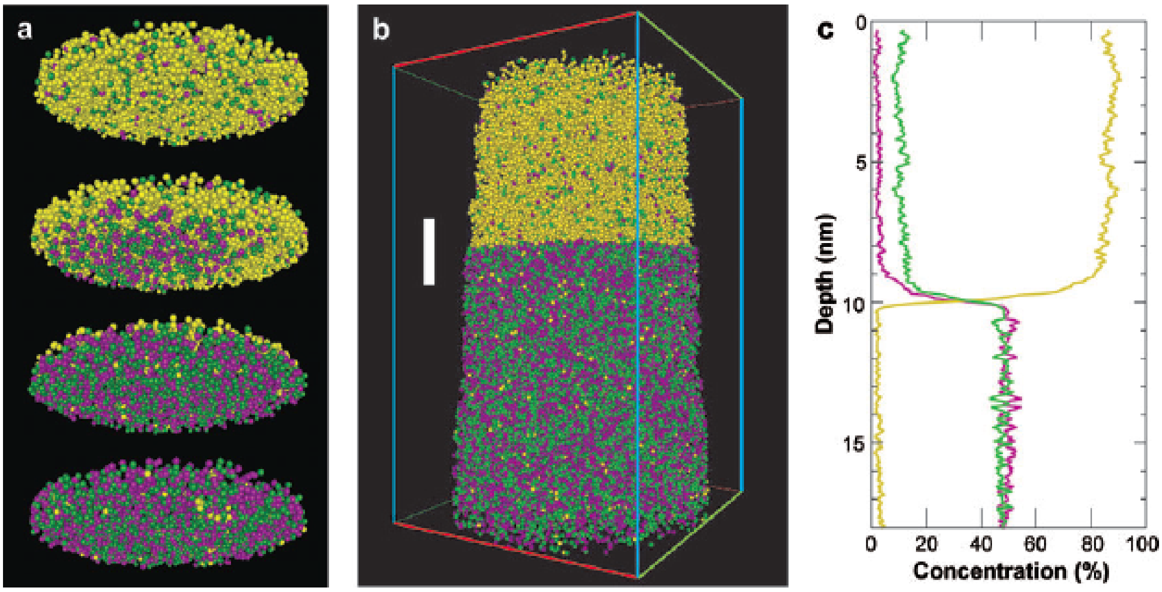

Figure 13

Catalyst nanowires interface in 3-D. (*a*) One-nm-thick slices through the nanowires over the region defined by the white bar in *b*. The diameter of the slices is 10 nm. In, As, and Au atoms are rendered as green, purple, and yellow dots, respectively. (*b*) A 14 × 14 × 23 nm^3 reconstruction of an InAs nanowire tip showing a Au catalyst particle at the top. (*c*) Composition profile in 1-D plotted along the growth axis and through the catalyst/nanowire interface. The plotted composition is a radially average value within a 4-nm-diameter cylinder centered in the middle of the nanowire. From Reference 121.